Kondo and crystal-field effects in the compound YbPtGa

D. T. Adroja and B. D. Rainford
Department of Physics, Southampton University, Southampton S09 5NH, United Kingdom

S. K. Malik
Tata Institute of Fundamental Research, Bombay 490 005, India

M. Gailloux and K. A. Gschneidner, Jr.
Ames Laboratory and Department of Materials Science and Engineering, Iowa State University, Ames, Iowa 50011
(Received 5 January 1994; revised manuscript received 4 April 1994)

The equiatomic ternary compound YbPtGa has been investigated by neutron diffraction, magnetic susceptibility, electrical resistivity, and low-temperature heat capacity measurements. A profile refinement of neutron diffraction data reveals that YbPtGa crystallizes in the orthorhombic TiNiSi-type structure. A λ-type anomaly is observed in the heat capacity at 3.8 K, and a broad maximum in the susceptibility is seen at 4 K, suggesting magnetic ordering of the Yb moment. The temperature dependence of the magnetic scattering resistivity exhibits a behavior consistent with Kondo-type interactions in the presence of crystalline electric field effects.

INTRODUCTION

In recent years there has been a great deal of interest in the magnetism of ternary equiatomic Kondo lattice compounds of the type RTX, where R=Ce and Yb, T is a transition metal and X is a metalloid.[1-8] These compounds have been reported to crystallize in a variety of different crystal structures, for example the cubic (MgAgAs type), hexagonal ($CaIn_2$, Fe_2P and GaGeLi types), tetragonal (LaIrSi type), orthorhombic (TiNiSi and $CeCu_2$ types),[9] etc. The factors which lead to the stabilization of a particular structure have not yet been established, though there is now a growing body of data. The crystal symmetry plays a central role in determining the magnetic properties, through the effects of the crystalline field (CF) acting on the orbital angular momentum of the $4f$ ions. The magnetic and transport properties of some of these compounds have been studied by our group and others.[1-8] These studies show that many of these compounds exhibit a variety of interesting ground-state properties, such as ferromagnetic Kondo lattice behavior in CePdSb and YbNiSn,[3,8] insulating Kondo lattice ground states in CeRhSb and CeNiSn,[1,2] and heavy fermion behavior in YbPdSb and YbPtBi.[6,7] As a part of a systematic investigation of the physical properties of RTX compounds, we have studied YbPtGa. Here we report the results of neutron diffraction, magnetic susceptibility, electrical resistivity, and heat capacity measurements on this compound. Neutron diffraction measurements show that YbPtGa crystallizes in the orthorhombic TiNiSi-type structure. Resistivity, magnetic susceptibility, heat capacity, and neutron scattering measurements reveal that YbPtGa is an antiferromagnetic Kondo lattice compound with a Néel temperature (T_N) of 3.8 K.

EXPERIMENT

The compound YbPtGa was prepared by arc melting the constituent elements, Yb (99.9% pure), Pt, and Ga (99.99%), which were obtained from commercial sources, on a water-cooled copper hearth under a high-purity argon atmosphere. Due to the volatile nature of Yb, a small excess of this constituent was used during the initial melt; this was found to be lost by the final melt. Powder x-ray-diffraction measurements were carried out using a Siemens diffractometer. Electron probe microanalysis was carried out, after polishing the sample surface by fine emery paper, using a JEOL scanning electron microscope (Model JSM-6400). Neutron-diffraction measurements were carried out on the time-of-flight LAD diffractometer at the ISIS Pulsed Neutron Facility, Rutherford Appleton Laboratory, UK: data were collected at seven different scattering angles between 4° and 150°. Resistivity measurements were carried out using a standard dc four-probe technique between 4.2 and 300 K. Magnetic susceptibility measurements were carried out using a vibrating sample magnetometer between 1.8 and 300 K. Magnetization-field isotherm measurements at 1.7 K were performed up to an applied field of 12 T. Low-temperature heat capacity measurements were made using an adiabatic heat pulse type calorimeter.[10]

RESULTS AND DISCUSSION

Our x-ray powder diffraction pattern for YbPtGa could be indexed entirely on the basis of an orthorhombic TiNiSi-type structure, space group *Pnma*, in agreement with a previous report.[9] No evidence of impurity phases was observed in the diffraction pattern. Optical microscopy clearly showed that the sample contained about

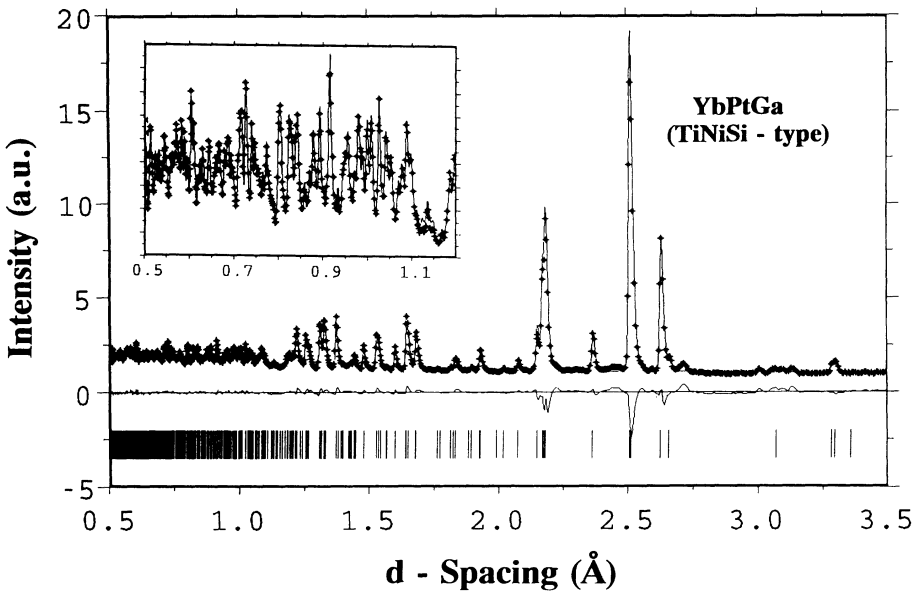

FIG. 1. Neutron diffraction pattern of YbPtGa at 300 K. Crosses are experimental points, and the lines show the calculated profile and the residuals.

10% of other phases. The microstructure showed islands of the YbPtGa primary phase surrounded by an apparent eutectic mixture of two phases of unknown composition. An electron microprobe analysis indicated that the primary phase had the nominal 1:1:1 composition. The orthorhombic TiNiSi-type structure is closely related to the orthorhombic $CeCu_2$-type structure (space group *Imma*). In the latter structure there are two different crystallographic sites, while the former structure has three crystallographic sites. A subdivision of the crystallographic 8*h* site (occupied by the Cu atoms) of the $CeCu_2$ structure into two 4*c* sites, by the preferential occupation of two distinct kinds of atoms, gives the TiNiSi-type structure. Rietveld profile analysis of the neutron diffraction data was used to confirm the space-group and site occupancies of YbPtGa. Figure 1 shows the neutron diffraction patterns obtained with the *LAD* diffractometer at a scattering angle of 150° at 300 K. The diffraction patterns were analyzed starting with two types of structures: (i) the orthorhombic TiNiSi type, in which Yb, Pt, and Ga atoms occupy distinct crystallographic 4*c* sites: $(x,\frac{1}{4},z)$, $(-x,\frac{3}{4},-z)$, $(\frac{1}{2}-x,\frac{3}{4},\frac{1}{2}+z)$, and $(\frac{1}{2}+x,\frac{1}{4},\frac{1}{2}-z)$; and (ii) the orthorhombic $CeCu_2$-type structure, in which the Yb atoms occupies the 4*e* sites $(0,\frac{1}{4},z_{Yb})$ and $(0,\frac{3}{4},z_{Yb})$, whereas the Pt and Ga atoms randomly occupy the 8*h* sites $(0,y,z)$, $(0,-y,-z)$, $(0,\frac{1}{2}+y,-z)$, and $(0,\frac{1}{2}-y,z)$. The refinement of the parameters was carried out in five stages: in the first stage background and cell parameters were estimated, while in the second stage peak shape parameters were refined. The refinement of the position parameters was carried out in the third stage. Isotropic temperature factors were refined in the fourth stage. All parameters were allowed to vary in the final state of the refinement. The value of the weighted profile factor R_{wp} obtained for the TiNiSi structure is 3.79%, while that for the $CeCu_2$, structure is 8.48%. This confirms that YbPtGa crystallizes in the orthorhombic TiNiSi-type structure. The values of the parameters obtained from the refinement for TiNiSi-type structure are given in Table I. The quality of the fit may be seen from the calculated profile, shown as a continuous line in Fig. 1, and the residuals, which are also shown.

Figure 2 shows the heat-capacity data, plotted as the ratio of heat capacity to temperature C/T versus T for YbPtGa. A λ-type anomaly is observed at 3.8 K: this is close to the temperature at which the magnetic susceptibility has a broad maximum (see the inset of Fig. 6). These features are taken to indicate magnetic ordering of the Yb moments: this has been shown to be antiferromagnetic by neutron diffraction measurements at 1.7 K.[11] The magnetic entropy S_m associated with the cooperative anomaly was calculated as follows: an estimate of the electronic contribution (γT) and phonon contribution (βT^3) to the heat capacity was made for the data in the temperature range above 12 K, using a linear extrapolation on a C/T versus T^2 plot. The value of γ and β obtained from a least-squares fit are 107 mJ/mole $K^2$and 0.608 mJ/mole K^4, respectively. This value of β yields a Debye temperature of 212 K, which is in agreement with the value of 209 K for LaNiIn.[12] The electronic and phonon contribution were then subtracted from the total

TABLE I. Refined atomic coordinates (x,y,z), lattice parameters (a,b,c), and isotropic temperature factors (ITF) for YbPtGa with TiNiSi-type structure (space group *Pnma*).

	x	y	z	ITF (Å^2)
Yb	−0.0127(3)	0.2500	0.6977(2)	0.0238(0.02)
Pt	0.2254(1)	0.2500	0.1003(5)	0.0370(0.03)
Ga	0.3280(1)	0.2500	0.4257(3)	0.0370(0.03)
a (Å)		6.730 28(6)		
b (Å)		4.345 11(4)		
c (Å)		7.584 440(7)		
R_{wp}		3.79%		

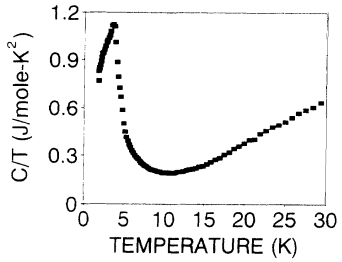

FIG. 2. Heat capacity of YbPtGa plotted as C/T vs T.

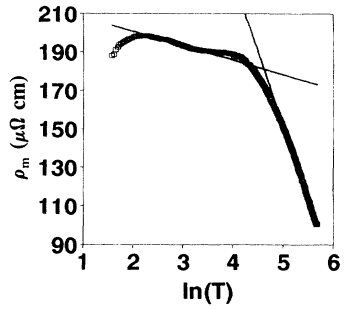

FIG. 4. Magnetic scattering resistivity vs temperature for YbPtGa.

heat capacity to give the magnetic contribution C_m, and S_m was estimated by numerical integration of a C_m/T versus T plot. A simple linear extrapolation was used to extend this plot from 2 K to zero temperature. The value found for S_m was 4.3 J/mole K per Yb ion, which is roughly 75% of R ln(2) (=5.76 J/mole per Yb ion), the value of the entropy expected to be associated with a doublet ground state. This procedure for calculating S_m is not entirely reliable, and the estimate may well be in error by 10–20%; however, it serves as a useful guide to the ground-state degeneracy: a crystal field double state is expected for the low point symmetry of YbPtGa. This has been confirmed by an inelastic neutron-scattering study of YbPtGa,[11] which reveals three CF transitions at 13.2, 25.5, and 45 meV, corresponding to transitions from the ground state to three excited doublets.

Figure 3 shows the resistivity of YbPtGa as a function of temperature between 5 and 300 K. The resistivity of the isostructural compound LaPtGa was also measured, in order to estimate the phonon contribution to the resistivity of YbPtGa (Fig. 3). The resistivity of YbPtGa increases with decreasing temperature from 300 K, and exhibits a broad maximum at 90 K. Below 90 K, the resistivity decreases with temperature and exhibits a minimum at 25 K, followed by a sharp drop at 8 K. The latter temperature is somewhat higher than the Néel temperature (3.8 K), deduced from heat capacity and susceptibility measurements. We attribute the drop in the resistivity at 8 K to either a substantial degree of magnetic short-range order or to the onset of coherence among the Yb moments. The magnetic scattering resistivity ρ_m obtained by subtracting the resistivity of LaPtGa from the resistivity of YbPtGa is shown in Fig. 4. $\rho_m(T)$ exhibits a $-\ln(T)$ dependence in two different temperature regimes, separated by a broad maximum. The observed behavior of $\rho_m(T)$ can be understood on the basis of the theory of Cornut and Coqblin,[13] who treated the problem of resistivity of single Kondo impurities in the presence of crystalline electric fields.[13] According to this theory, the $-\ln(T)$ behavior in the different temperature regimes is associated with the change in the population of the crystal-field split levels. In the limiting cases when $T \ll \Delta$ and $T \gg \Delta$, where Δ is the overall CF splitting, the ratio of the low-temperature $-\ln(T)$ slope to that at high temperature is given by $(\alpha_l^2-1)/(\alpha_h^2-1)$, where α_l and α_h are the low- and high-temperature degeneracies of the CF levels. Thus for a Yb ion having a doublet ground state and eightfold degeneracy at 300 K, the ratio of the slopes should be $1/21=0.0476$. The observed ratio is 0.09, which is higher than that predicted by theory. This discrepancy can be understood by considering the large value of the overall CF splitting (45 meV): at 300 K the highest-lying CF levels are not fully populated, so the effective degeneracy of the Yb ion is closed to 6 rather than 8. This would gives a ratio of the slopes $3/35=0.086$, which agrees well with the experimental value.

Figure 5 shows the magnetization isotherm of YbPtGa at 1.7 K. At a field of 12 T, the magnetization approaches saturation. The value of the saturation magnetic moment μ_s obtained by extrapolating M versus $1/H$ to $1/H \rightarrow 0$, is $1.55\mu_B$. Figure 6 shows the reciprocal magnetic susceptibility of YbPtGa as a function of temperature. Below 4 K the susceptibility exhibits a broad maximum (inset of Fig. 6), which is somewhat field depen-

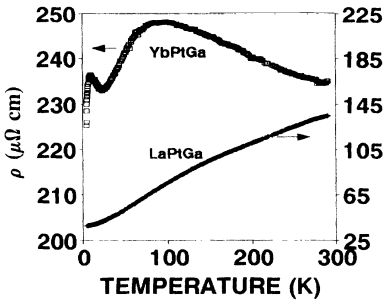

FIG. 3. Resistivity vs temperature for YbPtGa and LaPtGa.

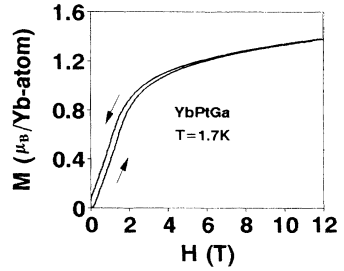

FIG. 5. Magnetization isotherm at 1.7 K for YbPtGa.

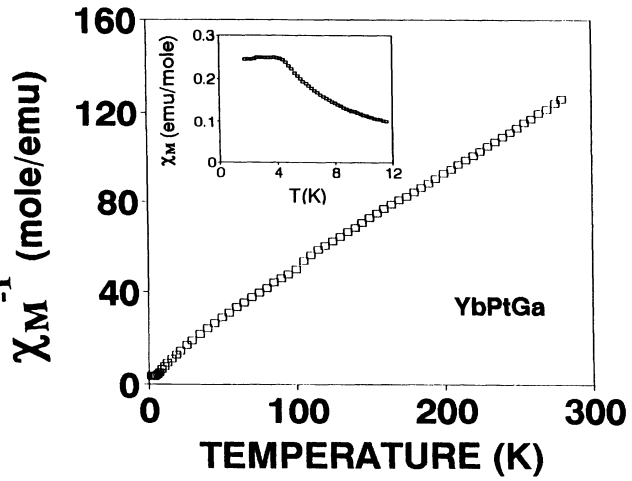

FIG. 6. Reciprocal magnetic susceptibility vs temperature for YbPtGa. The inset shows the magnetic susceptibility (in an applied field of 1 T) vs temperature.

dent. We have attributed this to antiferromagnetic ordering of the Yb moment. The susceptibility follows a Curie-Weiss behavior between 50 and 300 K, with an effective magnetic moment $\mu_{\text{eff}}=3.95\mu_B$ and a paramagnetic Curie temperature $\theta p=-23$ K. The observed value of μ_{eff} is smaller than $\mu_{\text{eff}}=4.52\mu_B$ of the free Yb^{3+} ion: again the reduction in μ_{eff} may be attributed to the large value of the overall CF splitting.

The Yb site in the TiNiSi structure has a low point symmetry. Analysis of the crystal field using the superposition model approach[14] shows that there are 15 independent CF parameters. Indeed terms like B_4^1 and B_4^3 appear to be of larger magnitude than terms with orthorhombic symmetry like B_4^2 and B_4^4 (the same is true for the sixth-order terms). Without single-crystal susceptibility data it is not possible to obtain a unique set of CF parameters including all the terms in the CF Hamiltonian. We will attempt to provide a fuller analysis of the crystal field in a future paper,[11] where the inelastic neutron scattering data for YbPtGa will be discussed in detail.

CONCLUSIONS

The profile refinement of neutron diffraction data confirms that YbPtGa crystallizes in the orthorhombic TiNiSi-type structure. Neutron scattering, heat capacity, and susceptibility measurements show that YbPtGa orders antiferromagnetically with a Néel temperature $T_N=3.8$ K. The temperature dependence of the magnetic scattering resistivity reveals the presence of Kondo and crystal-field interactions.

ACKNOWLEDGMENTS

This research was partially supported by the Science and Engineering Research Council (U.K.), and the office of Basic Energy Sciences, U.S. Department of Energy under Contract No. W-7405-ENG-82 at the Ames Laboratory, Iowa State University.

[1]T. Takabatake, F. Teshima, H. Fujii, S. Nishigori, T. Suzuki, T. Fujita, Y. Yamaguchi, J. Sukurai, and D. Jaccard, Phys. Rev. B **41**, 9607 (1990).
[2]S. K. Malik and D. T. Adroja, Phys. Rev. B **43**, 6277 (1991).
[3]S. K. Malik and D. T. Adroja, Phys. Rev. B **43**, 6295 (1991).
[4]M. Kasaya, T. Tani, K. Kawate, T. Mizashima, Y. Ishikawa, and K. Sato, J. Phys. Soc. Jpn. **60**, 3145 (1991).
[5]S. K. Malik, D. T. Adroja, S. K. Dhar, R. Vijayaraghavan, and B. D. Padalia, Phys. Rev. B **40**, 2414 (1989).
[6]S. K. Dhar, N. Nambudaripad, and R. Vijayaraghavan, J. Phys. F **18**, L41 (1988).
[7]Z. Fisk *et al.*, Phys. Rev. Lett. **67**, 3310 (1991).
[8]P. Bonville, P. Bellot, J. A. Hodges, P. Imbert, G. Jehanno, G. Le Bras, J. Hammann, and L. Leylekian, Physica B **182**, 105 (1992).
[9]E. Hovestreydt, N. Engel, G. Kleep, B. Chabot, and E. Parthe, J. Less-Common Met. **85**, 247 (1982).
[10]K. Ikeda, K. A. Gschneidner, Jr., B. J. Beaudry, and U. Atzmony, Phys. Rev. B **25**, 4604 (1982).
[11]B. D. Rainford and D. T. Adroja (unpublished).
[12]H. Fujii, T. Inoue, Y. Andoh, T. Takabatake, K. Satoh, Y. Maeno, T. Fujita, J. Sakurai, and Y. Yamaguchi, Phys. Rev. B **39**, 6840 (1989).
[13]B. Cornut and B. Coqblin, Phys. Rev. B **5**, 4541 (1972).
[14]D. J. Newman and B. Ng, Rep. Prog. Phys. **52**, 699 (1989).